FOIL METALLIZATION PROCESS FOR PERC SOLAR CELLS TOWARDS INDUSTRIAL FEASIBILITY

M. Graf[1*], D. Eberlein[1], H. Nagel[1], J. Nekarda[1], R. Böhme[2], A. Streek[3] and R. Preu[1]
[1]Fraunhofer Institute for Solar Energy Systems ISE, Heidenhofstraße 2, 79110 Freiburg, Germany
[2]InnoLas Solutions GmbH, Pionierstr. 6, 82152 Krailling, Germany
[3]University of Applied Sciences Mittweida, Technikumplatz 17, 09648 Mittweida, Germany

*Phone: +49 (0)761 4588 5055, e-mail: martin.graf@ise.fraunhofer.de

ABSTRACT: Aluminium foil in combination with laser fired contacts (*FolMet*) as rear side electrode for highly efficient passivated emitter and rear cells (PERC) has proven a high efficiency potential of up to 21.3 % using an optimized and simplified cell process. Two objectives towards industrialization are the acceleration of the laser process and the feasibility of module assembly. An ultrafast polygon scanning system and comprehensive simulations enabled process times $t_{\text{pro}} < 0.8$ s for 156x156 mm² wafers, which corresponds to an acceleration of processing speed by a factor of 20. An easy-to-apply possibility to realize the electrical interconnection between foil metallized cells, is the single-side coating of the aluminium foil using a special treatment. This process could be carried out before the foil attachment to the solar cell, which allows the usage of a fast and cheap role to role production tool. The created soldering pads are compatible with conventional interconnection techniques and modules assembled with this technique passed the humidity-freeze (HF10) and temperature-cycle (TC200) test successfully.

Keywords: laser processing, foil metallization, PERC

1 INTRODUCTION

Over the next two years the passivated emitter and rear cell (PERC) concept will be the new benchmark technology [1, 2]. The PERC contacting sequence for the rear side, which is rolled out at the moment, consists of three processes: local contact opening with laser (LCO), subsequently screen printing of aluminium paste and finally the fast firing for the contact formation [3]. One possible next generation technology for the rear side metallization, to further improve the cost effectiveness and energy conversion efficiency of PERC solar cells, can be the implementation of an aluminium foil electrode in combination with laser fired contacts (*FolMet*) [4, 5]. One advantage of the *FolMet* technology is the combination of the laser process and the metallization of the rear side in one single production machine, thus the contacting sequence is reduced to two processes: pulling foil over the wafer and lasering. No additional fast firing for the rear side contact formation is necessary. This technique has already proven a high efficiency potential of up to 21.3 % using an optimized, simplified and economical cell process [6]. Two objectives towards industrialization are the acceleration of the laser process and the compatibility with standard module assembly.

The purpose of this work is to further demonstrate the industrial feasibility of the *FolMet* technology. Therefore, a process time $t_{\text{pro}} < 1$ s is necessary with an optimized laser process and an ultra-fast scanning system for high speed laser beam delivery on the workpiece. A comprehensive simulation of the laser pulse aluminium foil interaction based on the finite differences method is used to gain a better understanding of the contact formation. Furthermore, we prove the module assembly with conventional soldering of the rear side foil metallization and the stability of the soldered interconnection during accelerated aging. We perform standard module testing, carrying out temperature-cycling (TC200) and humidity-freeze (HF10) tests.

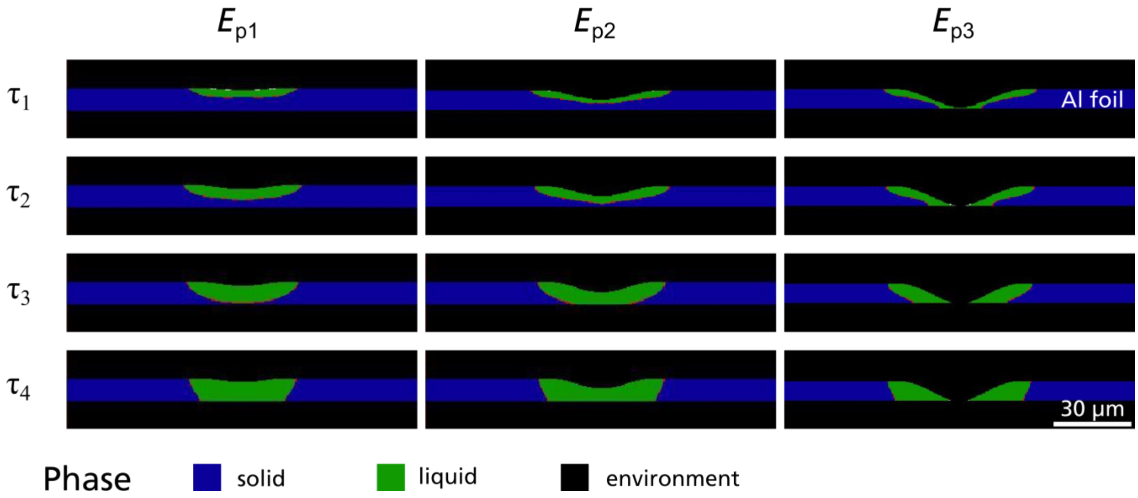

Figure 1: Phase diagram of the finite differences simulation results dependent on pulse energy E_p ($E_{p1} < E_{p2} < E_{p3}$) and pulse duration ($\tau_1 < \tau_2 < \tau_3 < \tau_4$)[7].

2 LASER PROCESS ACCELERATION

2.1 Development of single pass process

We start with a comprehensive simulation based on the finite differences method to better understand the interaction of pulse duration and pulse energy as previously reported [7, 8]. Accordingly we vary the pulse energy E_p with pulse durations in the nanosecond range, which can be emitted by a Jenoptik Jenlas IR70E laser system. The simulation results illustrate the phase changes during the process, as shown in Figure 1. The increase of the pulse duration leads to a higher melting depth for a constant pulse energy E_p1 (left column). One constraint for a successful contact formation is that molten aluminium permeates the whole 8 µm thick foil and reaches the solar cell rear side, which is applicable only for the longest pulse duration of the applied laser system in the case of E_p1. Increased pulse energies enable lower pulse durations as it can be seen for E_p2 in Figure 1, middle column. Another limitation is the wetting of the silicon surface with the molten aluminum. Without any additional surface pressure, the melt solidifies after cooling down devoid of creating any adhesion between foil and solar cell. Therefore the plasma plume of the evaporated material and the vaporized material, which create a repulsive force towards the solar cell, have to sustain until the melt reaches the interface between foil and solar cell to provide a proper wetting of the surface. With further increased pulse energy E_p3, material ablation dominates the process. As a result, for all simulated pulse durations, the entire aluminium in the contact area is evaporated and no material is left for surface wetting including contact formation.

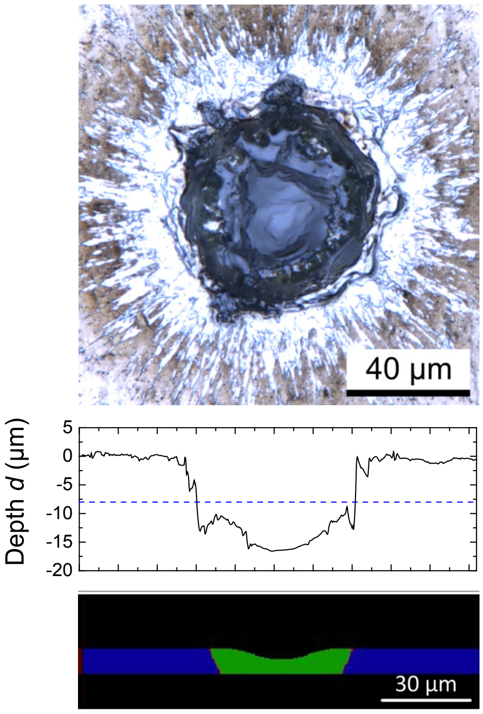

Figure 2: Comparison of the experimental and the simulated results for E_p2 and τ_3. Confocal microscopy image (top) and appropriate cross section of the contact (middle), the dashed blue line highlights the interface between foil and solar cell. Simulated forecast of the present phase at the maximum temperature (bottom)

For the experimental validation of this simulation, we use silicon wafers with a textured rear side, 20 nm aluminium oxide and 100 nm silicon nitride capping on top. The experimental result regarding the contact shape, as can be seen in the laser confocal microscopy image in Figure 2, shows good agreement with the simulation. However, the depth d of the contact differs somewhat, we assume this to be due to the neglected fluid dynamics of the molten aluminium in the finite differences simulation. With the aid of the simulation we could successfully implement a single pass laser process, decreasing the process time by a factor of three, compared to the current process.

2.2 Improvement of laser beam delivery on workpiece

Subsequently an ultrafast two dimensional polygon scanner (Figure 3), allowing a maximum scanning speed $v_\mathrm{scan} = 1000\ \mathrm{ms}^{-1}$, is used together with an IPG laser system, which is capable to reach high pulse repetition rates up to 2 MHz [9]. Due to the high scanning velocity, “long” lasting laser pulses lead to spatially elongated contacts. For that reason v_scan is limited to $250\ \mathrm{ms}^{-1}$. Hence, a processing time $t_\mathrm{pro} \sim 0.8\ \mathrm{s}$ per wafer is achieved, which is a factor of 20 lower compared to common scanning technology based on galvo driven mirrors.

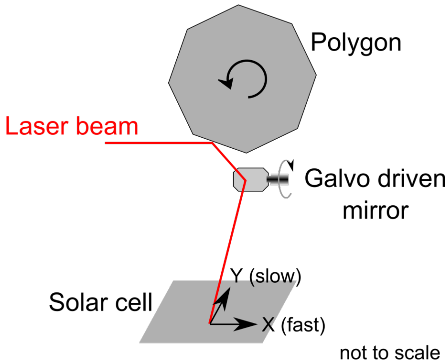

Figure 3: Scheme of a polygon scanner system [7].

3 MODULE ASSEMBLY

3.1 Soldering of aluminium foil

Due to a thin native oxide layer on every aluminium surface in the atmosphere, no sufficient wetting with solder can be achieved and therefore conventional soldering is impossible. An easy-to-apply possibility to realize the electrical interconnection between aluminium foil metallized cells, is the single-side coating of the foil using a special treatment or physical vapour deposition (PVD) method [10]. This process can be carried out before the foil attachment to the solar cell, which allows for a fast and cost-effective role to role production tool. The created soldering pads are compatible with conventional interconnection techniques. Hereinafter, we present only our results regarding the special coating technique. The cells are soldered manually using standard copper ribbons with solder coating. For the lamination process, we use a standard glass front side, ethylene-vinyl acetate (EVA) as embedding material and a transparent back sheet, enabling a narrow optical inspection of the rear side after lamination and module testing. Figure 4 shows the successfully assembled module composed of four *FolMet* solar cells.

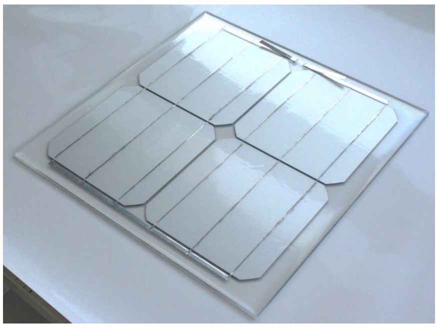

Figure 4: Four *FolMet* solar cells assembled to a small scale module with conventional soldering technique, enabled by a special foil treatment.

3.2 Accelerated aging of modules

After soldering and lamination, the modules (four and single cell modules) go through different accelerated aging tests, which are humidity-freeze for 10 cycles (HF10) and temperature-cycle for 200 cycles (TC200) according to IEC 61215. Before HF10 and TC200 testing, the modules are exposed to a light intensity of 0.2 suns for 36 h and a temperature $T < 40°C$ to fully activate the light induced degradation (LID) in the Cz-Si based modules. This preconditioning avoids a parasitic error during the accelerated aging procedure caused by LID. To measure the impact of the reliability tests, electroluminescence (EL) and *I-V* measurements are carried out initially and at the end of each test.

As can be seen in Figure 5 the EL image after HF10 (right) shows only minor changes in intensity compared to the initial image (left). The *I-V* testing of the initial module performance at the maximum power point $P_{\mathrm{MPP,\,initial}} = 16.0$ W and after HF10 $P_{\mathrm{MPP,\,HF10}} = 16.0$ W validates the EL results. A maximum power decrease of 5 $\%_{\mathrm{rel}}$ must not be exceeded to pass the accelerated aging test, therefore this manually produced module passed HF10 successfully.

Additional TC200 climatic chamber tests are carried out with single cell modules. The *I-V* results are shown in Table I before and after the accelerated aging. As mentioned earlier, the relative deviation should be less than $5\%_{\mathrm{rel}}$ to pass the TC200 test. We observe a fill factor decrease $\Delta FF = -1.4\%_{\mathrm{rel}}$, due to a slight increase in serial resistance. In addition, the open circuit voltage of the module declines by $\Delta V_{\mathrm{OC}} = -0.7\%_{\mathrm{rel}}$. Overall the power P_{MPP} decreases only $-2.2\%_{\mathrm{rel}}$, concluding the TC200 test is passed by that module. In summary, it can be stated that the *FolMet* technology in combination with the special treatment is capable to pass the previously shown accelerated aging tests.

Table I: *I-V* results of a single cell module before and after TC200

	P_{MPP} (W)	*FF* (%)	V_{OC} (mV)
Initial	4.33	75.08	632.8
TC200	4.23	74.00	628.6
Relative deviation (%)	-2.2	-1.4	-0.7

4 CONCLUSION

We have achieved an in-depth understanding of the Al foil based contacting process and we were able to accelerate the processing time per wafer to become industrial feasible, due to the finite differences simulation. We decreased the processing time to ~ 0.8 s per wafer by combining a single pass laser process with an ultrafast polygon scanner system. Furthermore, the compatibility of the roll to roll coated aluminium foil, with conventionally soldering techniques has been shown. First reliability tests, especially the temperature-cycle test, have been passed successfully with manually produced small scale modules. These tests are a part of the IEC 61215 certification. Applying a coated foil is a cost-efficient and easy way to provide full compatibility with conventional module assembly, devoid of any negative influence on the laser process.

5 ACKNOWLEDGMENT

The German Ministry for the Environment, Nature Conservation and Nuclear Safety (BMU) is gratefully acknowledged for financially supporting this work within the project: FolMet (contract number 0325574A). The authors also would like to thank all colleagues at Fraunhofer ISE who have contributed to this paper in general.

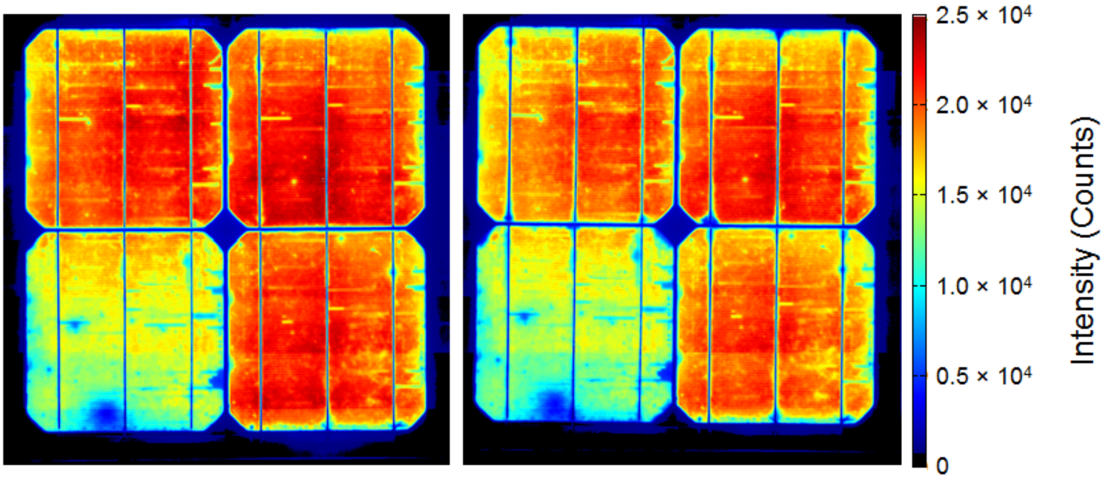

Figure 5: Electroluminescence (EL) images of a four cell module initial (left) and after HF10 (right) test.

6 REFERENCES

[1] A. W. Blakers, A. Wang, A. M. Milne, J. Zhao, and M. A. Green, “22.8% efficient silicon solar cell,” *Appl. Phys. Lett,* vol. 55, no. 13, pp. 1363–1365, 1989.

[2] J. Gifford, *CEO interview: Innovations in solar technology; PERC the new PV benchmark.* Available: http://www.pv-magazine.com/news/details/beitrag/ceo-interview--innovations-in-solar-technology-perc-the-new-pv-benchmark_100019981 (2015, Sep. 02).

[3] G. Agostinelli, J. Szlufcick, P. Choulat, and G. Beaucarne, “Local contact structures for industrial perc-type solar cells,” in *Proceedings of the 20th European Photovoltaic Solar Energy Conference and Exhibition*, 2005, pp. 942–945.

[4] E. Schneiderlöchner, R. Preu, R. Lüdemann, S. W. Glunz, and G. Willeke, “Laser-fired contacts (LFC),” in *Proceedings of the 17th European Photovoltaic Solar Energy Conference and Exhibition*, 2001, pp. 1303–1306.

[5] J. Nekarda, A. Grohe, O. Schultz, and R. Preu, “Aluminum foil as back side metallization for LFC cells,” in *Proceedings of the 22nd Europea Photovoltaic Solar Energy Conference and Exhibition*, 2007, pp. 1499–1501.

[6] M. Graf, J. Nekarda, D. Eberlein, N. Wöhrle, R. Preu, R. Böhme, and T. Große, “Progress in laser-based foil metallization for industrial PERC solar cells,” in *Proceedings of the 29th European Photovoltaic Solar Energy Conference and Exhibition*, 2014, pp. 532–535.

[7] M. Graf, J. Nekarda, F. L. Togny, A. Streek, R. Böhme, and R. Preu, “Comprehensive Simulation and Acceleration of the Foil-metallization Laser Process,” *Energy Procedia*, vol. 77, pp. 694–700, 2015.

[8] A. Streek, “Laser-Micro-Sintering,” Dissertation, Dresden, 2015, to be published.

[9] A. Streek, R. Ebert, and H. Exner, “Innovative Fertigungstechnik, -verfahren und -planungsmethoden,” Oelsnitz, Germany, 2014.

[10] J. Kumm, H. Samadi, P. Hartmann, S. Nold, A. Wolf, and W. Wolke, “Development of temperature-stable, solderable PVD rear metallization for industrial silicon solar cells,” in *Proceedings of the 28th European Photovoltaic Solar Energy Conference and Exhibition*, 2013, pp. 1287–1290.